European Cells and Materials Vol. 23 2012 (pages 400-412) DOI: 10.22203/eCM.v023a31 ISSN 1473-2262

INJECTABLE SKELETAL MUSCLE MATRIX HYDROGEL PROMOTES NEOVASCULARIZATION AND MUSCLE CELL INFILTRATION IN A HINDLIMB ISCHEMIA MODEL

Jessica A. DeQuach[1], Joy E. Lin[1], Cynthia Cam[1], Diane Hu[1], Michael A. Salvatore[1], Farah Sheikh[2] and Karen L. Christman[1]*

[1]Department of Bioengineering, University of California, San Diego, La Jolla, CA, USA
[2]Department of Medicine, University of California, San Diego, La Jolla, CA, USA

Abstract

Peripheral artery disease (PAD) currently affects approximately 27 million patients in Europe and North America, and if untreated, may progress to the stage of critical limb ischemia (CLI), which has implications for amputation and potential mortality. Unfortunately, few therapies exist for treating the ischemic skeletal muscle in these conditions. Biomaterials have been used to increase cell transplant survival as well as deliver growth factors to treat limb ischemia; however, existing materials do not mimic the native skeletal muscle microenvironment they are intended to treat. Furthermore, no therapies involving biomaterials alone have been examined. The goal of this study was to develop a clinically relevant injectable hydrogel derived from decellularized skeletal muscle extracellular matrix and examine its potential for treating PAD as a stand-alone therapy by studying the material in a rat hindlimb ischemia model. We tested the mitogenic activity of the scaffold's degradation products using an *in vitro* assay and measured increased proliferation rates of smooth muscle cells and skeletal myoblasts compared to collagen. In a rat hindlimb ischemia model, the femoral artery was ligated and resected, followed by injection of 150 μL of skeletal muscle matrix or collagen 1 week post-injury. We demonstrate that the skeletal muscle matrix increased arteriole and capillary density, as well as recruited more desmin-positive and MyoD-positive cells compared to collagen. Our results indicate that this tissue-specific injectable hydrogel may be a potential therapy for treating ischemia related to PAD, as well as have potential beneficial effects on restoring muscle mass that is typically lost in CLI.

Keywords: Muscle; extracellular matrix; hydrogel; tissue engineering; scaffold.

*Address for correspondence:
Karen L. Christman
Department of Bioengineering
2880 Torrey Pines Scenic Dr.
University of California, San Diego,
La Jolla, CA, USA

Telephone Number: 1-858 822-7863
Fax Number: 1-858 534-5722
E-mail: christman@bioeng.ucsd.edu

Introduction

Peripheral artery disease (PAD) is a common condition in which blood flow is reduced to the legs and feet (Manzi *et al.*, 2011; Stansby and Williams, 2011). Critical limb ischemia (CLI) is the most advanced form of PAD, often leading to amputation of the limb and potential mortality (Chan and Cheng, 2011; Dattilo and Casserly, 2011). The only current clinical treatment for PAD and CLI is endovascular or surgical revascularization (Dattilo and Casserly, 2011). Surgical bypass was the established standard, but recently endovascular therapies such as angioplasty, atherectomy and stenting are used as less-invasive options. However, despite these therapies, CLI continues to carry a major risk of limb amputation, with rates that have not changed significantly in 30 years (Tongers *et al.*, 2008).

Recently, several clinical trials using cell therapy have demonstrated promising results (Alev *et al.*, 2011; Gupta and Losordo, 2011; Kawamoto *et al.*, 2009; Menasché, 2010), but there are still many questions about which therapeutic cell type to use, quantity of cells, and best route to deliver the cells, as well as a significant problem with poor cell retention and survival (Menasché, 2010). Biomaterial scaffolds have more recently been explored to enhance cell survival by providing a temporary mimic of the extracellular matrix (ECM) (Kawamoto *et al.*, 2009; Layman *et al.*, 2011). Biomaterials have also been used for delivery of growth factors or their mimics in animal models of PAD and CLI (Kawamoto *et al.*, 2009; Layman *et al.*, 2011; Ruvinov *et al.*, 2010; Webber *et al.*, 2011). However, these scaffolds are composed of fibrin (Layman *et al.*, 2011), collagen-based matrix (Kuraitis *et al.*, 2011), gelatin (Layman *et al.*, 2007), self-assembling peptide amphiphiles (Webber *et al.*, 2011) or alginate (Ruvinov *et al.*, 2010), which may not provide the proper biomimetic environment for the ischemic skeletal muscle in these conditions. Moreover, no potential therapies employing only a biomaterial have been explored to date. An acellular, biomaterial only approach may reach the clinic sooner since it has the potential to be an off-the-shelf treatment and does not have the added complications that cells bring, including appropriate source, the need for expansion, or potential disease transmission. Furthermore, a biomaterial that promotes neovascularization and tissue repair on its own would obviate the need for exogenous growth factors, and the difficulties and expense associated with such a combination product.

The ECM of each tissue contains similar components; however, each individual tissue is composed of a unique combination of proteins and proteoglycans (Lutolf

and Hubbell, 2005; Uriel *et al.*, 2009). Recent studies have shown that the ECM of various tissues can be isolated through decellularization and utilized as a tissue engineering scaffold (Merritt *et al.,* 2010; Ott *et al.*, 2008; Singelyn *et al.*, 2009; Uygun *et al.*, 2010; Valentin *et al.*, 2010; Young *et al.*, 2011). Thus, for treating critical limb ischemia, using decellularized skeletal muscle matrix would provide the best mimic of the native ECM's biochemical cues, and was therefore explored in this study. Other decellularized ECM materials have been used for a variety of applications for tissue repair (Crapo *et al.*, 2011; Gilbert *et al.*, 2006). These scaffolds are known to promote cellular influx in a variety of tissues (Numata *et al.*, 2004; Rieder *et al.*, 2006). Their degradation products have angiogenic (Li *et al.*, 2004) and chemoattractant (Badylak *et al.*, 2001; Beattie *et al.*, 2008; Li *et al.*, 2004; Zantop *et al.*, 2006) properties, and also promote cell migration and proliferation (Reing *et al.*, 2009). After removal of the cellular antigens, these scaffolds are considered biocompatible, and both allogeneic and xenogeneic ECM devices have been approved by the FDA and are in clinical use (Badylak, 2007). A decellularized skeletal muscle scaffold has been previously explored for replacement of a muscle defect (Merritt *et al.,* 2010; Wolf *et al.*, 2012), yet this intact scaffold would not be amenable to treating peripheral artery disease. We, therefore, sought to develop an injectable hydrogel derived from skeletal muscle matrix that would allow for minimally invasive delivery and treatment of PAD and CLI.

We have recently developed hydrogels derived from decellularized ECMs, including myocardium (Singelyn *et al.*, 2009), pericardium (Seif-Naraghi *et al.*, 2010), and adipose tissue (Young *et al.*, 2011), which assemble into porous and fibrous scaffolds upon injection *in vivo.* We have recently shown that the injectable hydrogel derived from ventricular ECM promoted endogenous cardiomyocyte survival and preserved cardiac function post-myocardial infarction (Singelyn *et al.*, 2012). In this study, we developed an analogous tissue-specific hydrogel derived from skeletal muscle ECM and examined its potential as a biomaterial only therapy for treating PAD and CLI.

In previous studies, we have shown that a liquid form of skeletal muscle matrix, which forms the hydrogel in this study, was able to promote the differentiation and maturation of C2C12 skeletal myoblast progenitors when used as a cell culture coating (DeQuach *et al.*, 2010). We previously characterized this material, demonstrating its ability to retain a complex mixture of skeletal muscle ECM proteins, peptides, and proteoglycans (DeQuach *et al.*, 2010). In this study, we demonstrate that a liquid form of skeletal muscle matrix can assemble into a fibrous scaffold upon injection *in vivo*. The material can also be processed into a lyophilized form that only requires sterile water to resuspend prior to injection, which could provide ease of use in a clinical setting. We show that this injectable skeletal muscle material promotes proliferation of vascular cells and muscle progenitors *in vitro*, and that the hydrogel enhances neovascularization as well as the infiltration of muscle progenitors and proliferating muscle cells *in vivo* in a hindlimb ischemia model, thereby demonstrating its potential for treating PAD and CLI by not only treating ischemia, but also promoting tissue repair.

Materials and Methods

All experiments in this study were performed in accordance with the guidelines established by the Committee on Animal Research at the University of California, San Diego and the American Association for Accreditation of Laboratory Animal Care.

Decellularization of skeletal muscle for matrix preparation

Skeletal muscle from the hindleg was harvested from Yorkshire pigs, approximately 30-45 kg, immediately after sedation with a ketamine/xylazine combination (25 mg/kg, 2 mg/kg, respectively) and euthanasia with beuthanasia (1 mL/5 kg). Fat and connective tissue was removed, and the skeletal muscle was cut into ~1 cm^3 pieces and decellularized as previously published (DeQuach *et al.*, 2010). Briefly, the tissue was rinsed with deionized water and stirred in 1 % (wt/vol) solution of sodium dodecyl sulfate (SDS) in phosphate-buffered saline (PBS) for 4-5 d. Decellularized skeletal muscle was stirred overnight in deionized water and then agitated rinses under running deionized water were performed to remove residual SDS. A sample of decellularized matrix was frozen in Tissue Tek O.C.T. freezing medium, sectioned into 10 µm slices, and stained with hematoxylin and eosin (H&E) to confirm the absence of nuclei. Following the decellularization protocol, the ECM was lyophilized overnight and milled to a fine powder using a Wiley Mini Mill (Thomas Scientific, Swedesboro, NJ, USA). Additionally, to quantify DNA content, the DNeasy assay (Qiagen, Valencia, CA, USA) was performed according to manufacturer's instructions. After extraction, the Take3 plate was used to measure the concentration of DNA using a Synergy 2 microplate reader (Biotek, Winooski, VT, USA).

Preparation of injectable skeletal muscle matrix and collagen

In order to render the decellularized extracellular matrix (ECM) into a liquid form, the milled form of the matrix was subjected to enzymatic digestion (DeQuach *et al.*, 2010; Singelyn *et al.*, 2009). Pepsin (Sigma, St. Louis, MO, USA) was dissolved in 0.1 M HCl to make a 1 mg/mL pepsin solution and then filtered through a 0.22 µm filter (Millipore, Billerca, MA, USA). The ECM at a ratio of 10:1 was digested in the pepsin solution under constant stirring. After approximately 48 h, the matrix was brought to a physiological pH in a BSL-2 safety cabinet, and then either diluted for *in vitro* assays or for injection. For *in vitro* and *in vivo* studies, the skeletal muscle matrix was brought to a pH of 7.4 through the addition of sterile-filtered NaOH and 10x PBS, and further diluted to 6 mg/mL using 1x PBS inside a BSL-2 safety cabinet (Singelyn *et al.*, 2009).

Skeletal muscle matrix *in vitro* gel characterization

Gels of the skeletal muscle matrix were formed at a concentration 6 mg/mL for rheological characteristics and

for scanning electron microscopy. Either 100 µL of matrix was pipetted into a 96 well plate (Corning, Corning, NY, USA) or 500 µL in glass scintillation vials and incubated overnight to form gels. Rheometry was conducted on the 500 µL *in vitro*-formed skeletal muscle matrix gels using an AR-G2 rheometer (TA Instruments, New Castle, DE, USA). The gels were tested using a 20 mm parallel plate geometry with a 1.2 mm gap at 37 °C. Three frequency sweeps were performed within the linear viscoelastic strain region. Samples were run in triplicate and then the values were averaged to calculate the storage modulus.

Scanning electron microscopy (SEM) was utilized to determine the microstructure of the skeletal muscle matrix gels. These gels were either formed *in vivo* by injecting the skeletal muscle matrix subcutaneously in a rat and excised after 20 min, or *in vitro* after incubation of the material in a 96 well plate at 37 °C overnight. The skeletal muscle matrix gels were harvested and fixed with 2.5 % glutaraldehyde for 2 h, and then dehydrated using a series of ethanol rinses (30-100 %). Samples were then critical point dried and coated with iridium using a Emitech K575X Sputter coater (Quorum, Hatfield, PA, USA). Electron microscopy images were taken using a Phillips XL30 Environmental SEM Field Emission microscope at 10 kV, with 242 µA and a working distance of 10 mm.

In vitro proliferation assays

Primary rat aortic smooth muscle cells (RASMC) and C2C12 skeletal myoblasts were maintained on collagen-coated plates and split at 1:5 every 2-3 d. Cells between passages 4 and 10 were plated at 750 cells/well in 96 well plates in growth medium consisting of DMEM, 10 % fetal bovine serum, and 1 % pen-strep solution. Twenty-four hours later, the cells were washed with PBS to remove non-adherent cells. Digested skeletal muscle matrix and collagen were brought to a pH of 7.4, and then added to the growth medium at concentrations of 0.05 mg/mL. Because the ECM was enzymatically digested, pepsin was also included as a control at 0.005 mg/mL. All conditions were run in quadruplicate. Every 2 d, medium was changed and cell proliferation was assessed using the Picogreen® assay (Invitrogen, Carlsbad, CA, USA)) per manufacturer's directions. Briefly, wells were rinsed in PBS and then incubated with 100 µL Tris/EDTA buffer. After incubation for 30 min at room temperature followed by 5 min on a shaker, 100 µL of 1:200 Picogreen reagent was added. Upon covering the plates in foil and shaking them for 30 min, double stranded DNA was quantified using a fluorescent plate reader at 630 nm at days 3, 5, and 7.

In vivo gelation test

To prepare for *in vivo* studies, a preliminary test was performed to ensure that the skeletal muscle matrix would be able to gel upon injection. The skeletal muscle matrix was labeled with biotin, and then injected into the hindlimbs of healthy Sprague Dawley rats. For biotin labeling, a 10 mM solution of EZ link Sulfo-NHS-Biotin (Pierce, Rockford, IL, USA) was prepared and mixed with the liquid skeletal muscle matrix for a final concentration of 0.3 mg biotin/mg matrix. The mixture was allowed to sit on ice for 2 h. The skeletal muscle matrix was then frozen, lyophilized and stored at -80 ºC until use. To resuspend the skeletal muscle matrix, sterile water was added at the original volume to bring the material to 6 mg/mL and vortexed. Female Harlan Sprague Dawley rats (225-250 g) were anesthetized using isoflurane at 5 %, intubated, and maintained at 2.5 % isoflurane during surgery. In preliminary studies, 150 µL of skeletal muscle matrix was injected intramuscularly into healthy rats ($n = 2$). The muscle was excised after 20 min, and fresh frozen using Tissue Tek O.C.T.

Hindlimb ischemia model

After confirmation of gelation *in vivo*, a rat hindlimb ischemia model was utilized to test the skeletal muscle extracellular matrix. Animals were placed in a supine position and hindlimb ischemia was induced by ligation and excision of the femoral artery. After ligation of the proximal end of the femoral artery, the distal portion of the saphenous artery was ligated and the artery and side branches were dissected free, and then excised as previously described (Bach *et al.*, 2006; Bhang *et al.*, 2011). The area was sutured closed and animals were given an analgesic of 0.05 mg/kg buprenorphine hydrochloride (Reckitt Benckiser Healthcare (UK) Ltd., Hull, England) prior to recovery from anesthesia. One week post-injury, the rats were anesthetized using 5 % isoflurane, intubated, and maintained at 2.5 % isoflurane for injection. Skeletal muscle matrix and rat tail collagen were biotinylated in order to visualize the injection region and 150 µL was injected intramuscularly. Injection was confirmed by a lightening of the muscle at the site of injection. Rats were sacrificed using an overdose of sodium pentobarbital (200 mg/kg) at 3, 5, 7 or 14 d post injection ($n = 4$, except $n = 3$ for 14 d collagen injection), and leg muscles were harvested and frozen in Tissue Tek O.C.T.

Histology and immunohistochemistry

The excised muscle was cryosectioned into 10 µm slices. Slices were stained with H&E every 1 mm and screened to determine the location of injected material. Adjacent slides were stained for visualization of biotin-labeled skeletal muscle matrix or collagen, to confirm the injection site. Slides were fixed in acetone, incubated with superblock buffer (Pierce), followed by 3 % hydrogen peroxide (Sigma), and horseradish peroxidase-conjugated neutravidin (Pierce, Rockford, IL, USA) at room temperature. The reaction was visualized by incubation with diaminobenzidine (DAB, Pierce) for 10 min.

Five slides evenly spaced within the injection region were then used for immunohistochemistry (IHC). Sections were fixed for 2 min in acetone and blocked with staining buffer for 1 h (2 % goat serum and 0.3 % Triton X-100 in PBS). Skeletal muscle sections were then assessed for vessel formation using a mouse anti-smooth muscle actin antibody (Dako, Carpinteria, CA, USA; 1:75 dilution) to label smooth muscle cells. After three 5-min washes with PBS, AlexaFluor 568 anti-mouse antibody (Invitrogen, 1:200 dilution) was used as a secondary antibody. Endothelial cell infiltration was assessed using FITC-labeled isolectin (Vector Laboratories, Burlingame, CA, USA; 1:100 dilution). Slides were then mounted

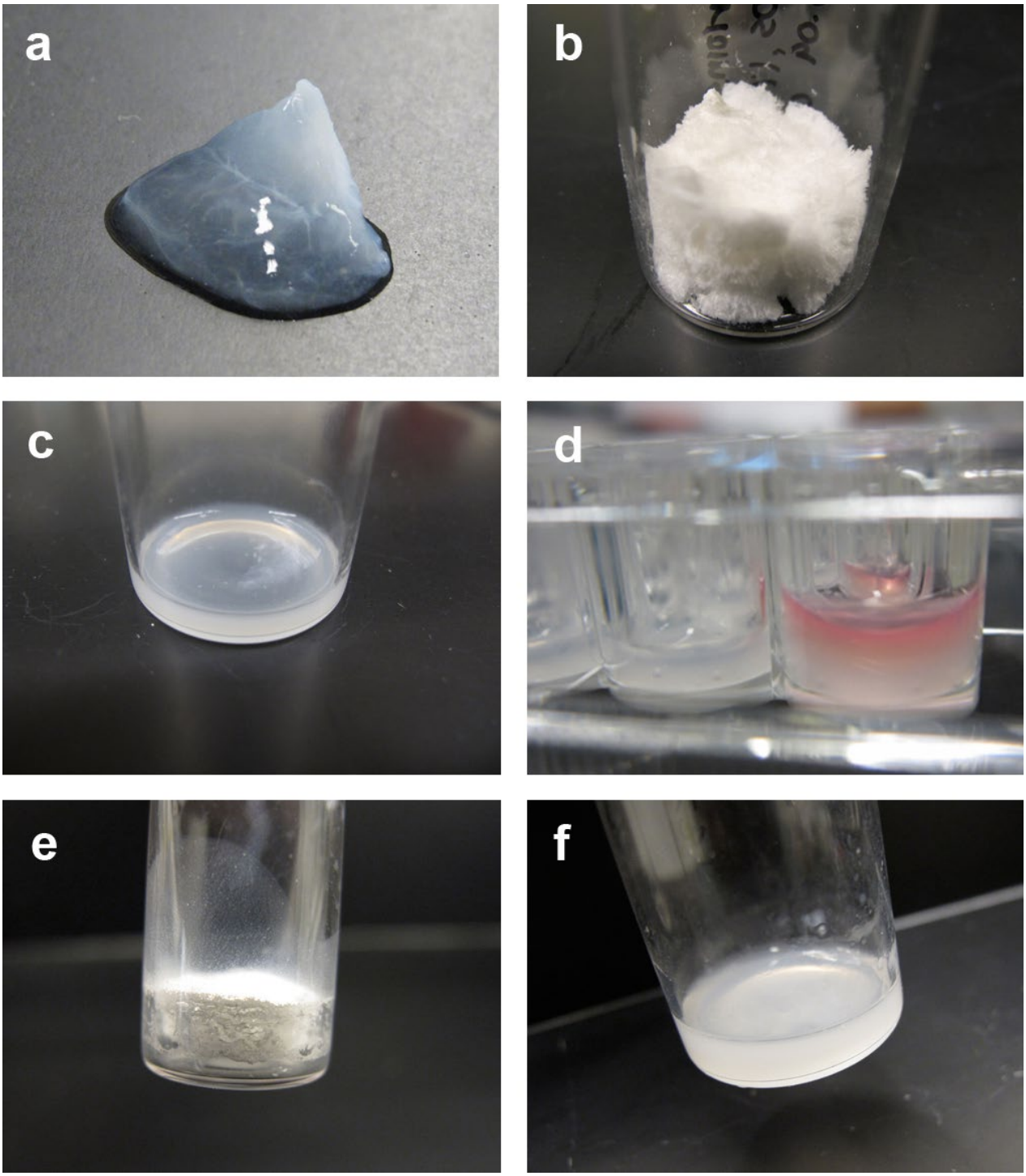

Fig. 1. Decellularization and tissue processing. **(a)** Decellularized skeletal muscle matrix. **(b)** Lyophilized skeletal muscle matrix prior to milling. **(c)** Digested skeletal muscle matrix. **(d)** *In vitro* gel of the skeletal muscle matrix with media on top in right well. **(e)** Skeletal muscle matrix that has been digested and re-lyophilized. **(f)** Re-lyophilized skeletal muscle matrix resuspended using only sterile water.

using Fluoromount (Sigma). Sections stained with only the primary antibody or secondary antibody were used as negative controls. Images were taken at 100x using Carl Zeiss Observer D.1 microscope (Zeiss, Thornwood, NY, USA) and analyzed using AxioVision software. Arterioles were quantified with a visible lumen and a diameter ≥ 10 μm and normalized over the injection area as previously described (Christman *et al.*, 2004; Singelyn *et al.*, 2009).

In order to assess proliferating muscle cell infiltration into the injection region, sections were stained using a mouse anti-desmin antibody (Sigma; dilution 1:100) and co-stained with a rabbit anti-Ki67 antibody (Santa Cruz Biotech, Santa Cruz, CA, USA; dilution 1:100). AlexaFluor 488 anti-mouse and AlexaFluor 568 anti-rabbit antibodies were used as secondary antibodies (1:200), followed by staining with Hoechst 33342. Slides were mounted with Fluoromount (Sigma) prior to imaging. Additionally, the

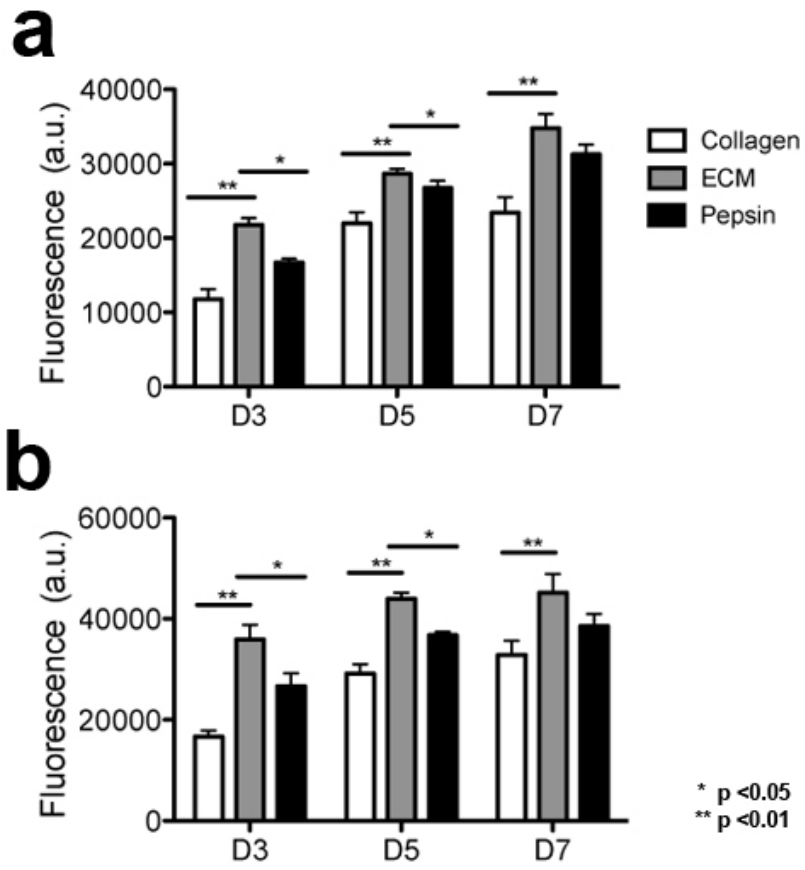

Fig. 2. *In vitro* mitogenic activity assay. **(a)** Rat aortic smooth muscle cells and **(b)** C2C12 skeletal myoblasts were cultured using growth medium with the addition of degraded skeletal muscle matrix, collagen, or pepsin. Proliferation rate was increased for both cell types when cultured in the presence of skeletal muscle matrix degradation products.

skeletal muscle tissue was assessed using a rabbit anti-MyoD antibody (Santa Cruz Biotech; dilution 1:100), followed by AlexaFluor 488 anti-rabbit antibody as a secondary antibody, and Hoechst 33342. Three 400x images were taken per slide and analyzed using AxioVision software. The number of desmin positive cells, and desmin positive cells that co-localized with Ki67 were counted, averaged and normalized over the area. For the tissue sections analyzed for MyoD, the number of positive cells with MyoD co-localized with nuclei were counted and averaged over the area of injection.

Statistical analysis

All data are presented as the mean ± standard error of mean. For the *in vitro* assays, samples were run in quadruplicate and results were averaged. Significance was determined using a one-way analysis of variance (ANOVA) with a Bonferroni post-test. A two-tailed Student's *t*-test was used for all other data and reported as $p < 0.05$ and $p < 0.01$.

Results

Injectable skeletal muscle matrix

Skeletal muscle matrix material was derived through decellularization of porcine skeletal muscle tissue (Fig. 1a) using previously established methods (DeQuach *et al.*, 2010). In addition to confirmation with lack of nuclei on H&E stained sections (not shown), the DNA content of the material was measured as 26.14 ± 1.67 ng of DNA/mg of dry weight ECM, which confirmed decellularization. The matrix was then lyophilized (Fig. 1b) and milled into a fine particulate before enzymatic digestion to form a liquid (Fig. 1c). At this stage, the liquid skeletal muscle matrix can be diluted and utilized as a coating for cell culture as we have previously reported (DeQuach *et al.*, 2010), or can be brought to physiological pH and temperature, which triggers assembly into a hydrogel (Fig. 1d). After raising the pH of the material to 7.4 at room temperature, the material can also be re-lyophilized (Fig. 1e) for long-term storage at -80 ºC. The material can then be resuspended at a later date using only sterile water (Fig. 1f) and utilized for *in vivo* injection.

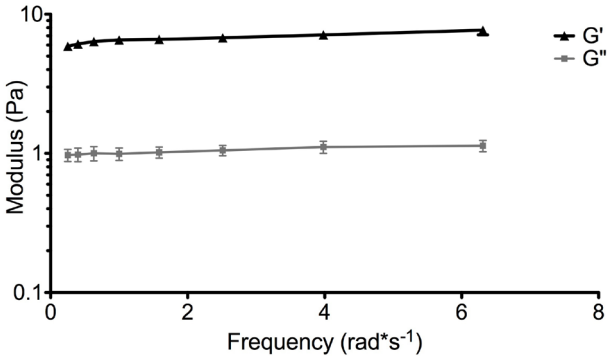

Fig. 3. Rheological data. A representative trace of the storage (G') and loss (G") moduli for the skeletal muscle matrix gel is shown.

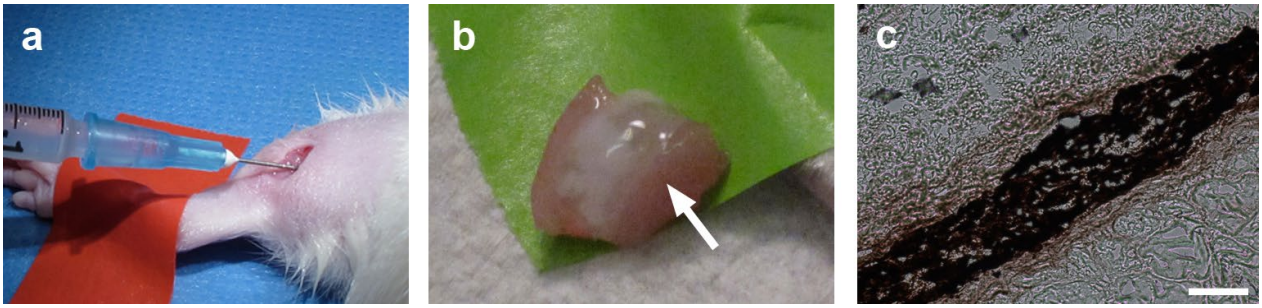

Fig. 4. Skeletal muscle matrix delivery and gelation *in situ.* **(a)** Intramuscular injection of the skeletal muscle matrix material. **(b)** Gelation of the skeletal muscle matrix *in situ* after 20 min as seen after excision of the muscle; arrow denotes the white matrix. **(c)** DAB staining of the biotin-labeled skeletal muscle matrix that gelled within the muscle. Scale bar at 200 μm.

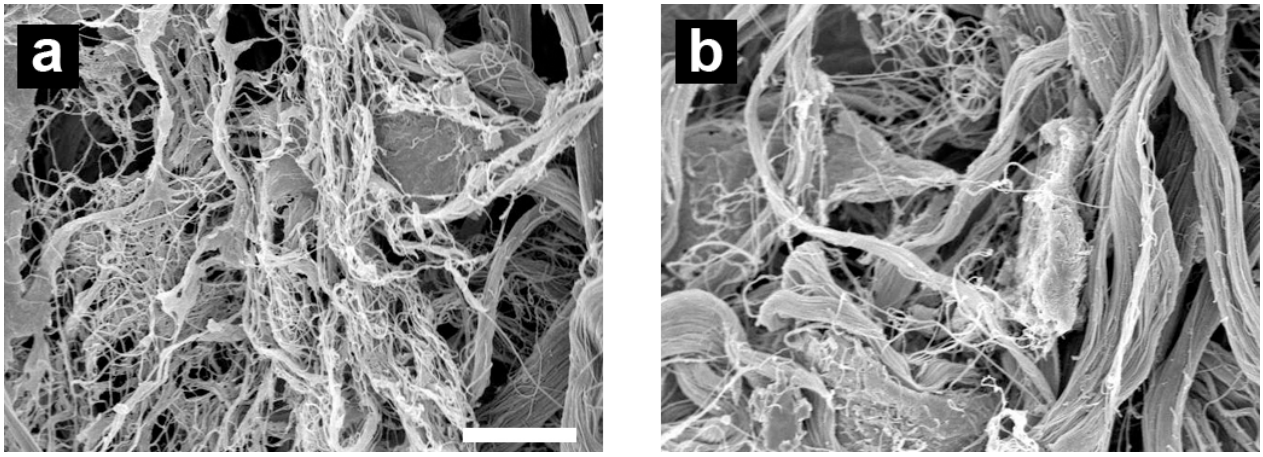

Fig. 5. Scanning electron microscopy. Micrograph of a cross-section of skeletal muscle matrix formed **(a)** *in vitro*, and **(b)** 20 min post-subcutaneous injection. Note the formation of the assembled fibers on the nano- and micro- scale. Scale bar at 100 μm.

Mitogenic assay

Degradation products of decellularized ECMs have been previously shown to have mitogenic activity (Reing *et al.*, 2009). We, therefore, first examined whether the degradation products of the skeletal muscle matrix hydrogel had a mitogenic effect on cells *in vitro*. Proliferation of smooth muscle cells and skeletal myoblasts following exposure to either enzymatically degraded skeletal muscle ECM or collagen was assessed. Pepsin was also included as a control, as pepsin was utilized to digest the matrix material. A Picogreen assay was used to determine double stranded DNA content at days 3, 5 and 7 in culture to quantify cell proliferation. It was found that both smooth muscle cells (Fig. 2a) and myoblasts (Fig. 2b), when cultured in media containing degraded skeletal muscle matrix, had a higher rate of proliferation compared to cells cultured in media containing the same concentration of collagen. The increase in cell number was significantly greater at all time points ($p < 0.01$). At day 3, there was a 1.85-fold increase in cell number in the skeletal muscle matrix wells compared to collagen for the smooth muscle cells, and a corresponding 2.15-fold increase with the skeletal myoblasts. There was also a 1.3-fold increase for skeletal muscle matrix wells compared to pepsin for both cell types, while the pepsin and collagen controls were not statistically different. Thus, degradation products of the skeletal muscle matrix were shown to promote mitogenic activity in both cell types *in vitro* when compared to collagen or the pepsin control.

Gelation *in vitro* and *in vivo*

We initially made a gel form of the matrix *in vitro* by bringing the material to a physiological pH and incubating the material at 37 °C. After gelation, the material was tested for rheological properties where it was determined that the material had a storage modulus (G') of 6.5 ± 0.5 Pa. A representative trace of rheological data is shown in Fig. 3. We then assessed the ability of the liquid skeletal muscle matrix to form a gel *in situ* by injecting the material into a healthy rat hindlimb. For all *in vivo* studies, we utilized liquid skeletal muscle matrix, which had been biotinylated and re-lyophilized for storage at -80 °C. Prior to injection, the material was resuspended in sterile water alone. The skeletal muscle matrix was then loaded into a syringe and injected intramuscularly into a rat hindlimb (Fig. 4a). To determine whether the skeletal muscle matrix would assemble and form a scaffold, the injection region was excised after 20 min. A visible gel, denoted by the white region in Fig. 4b, was observed within the muscle. Additional matrix injections were cryosectioned and stained to visualize the biotinylated matrix. Similar to our myocardial matrix hydrogel (Singelyn *et al.*,

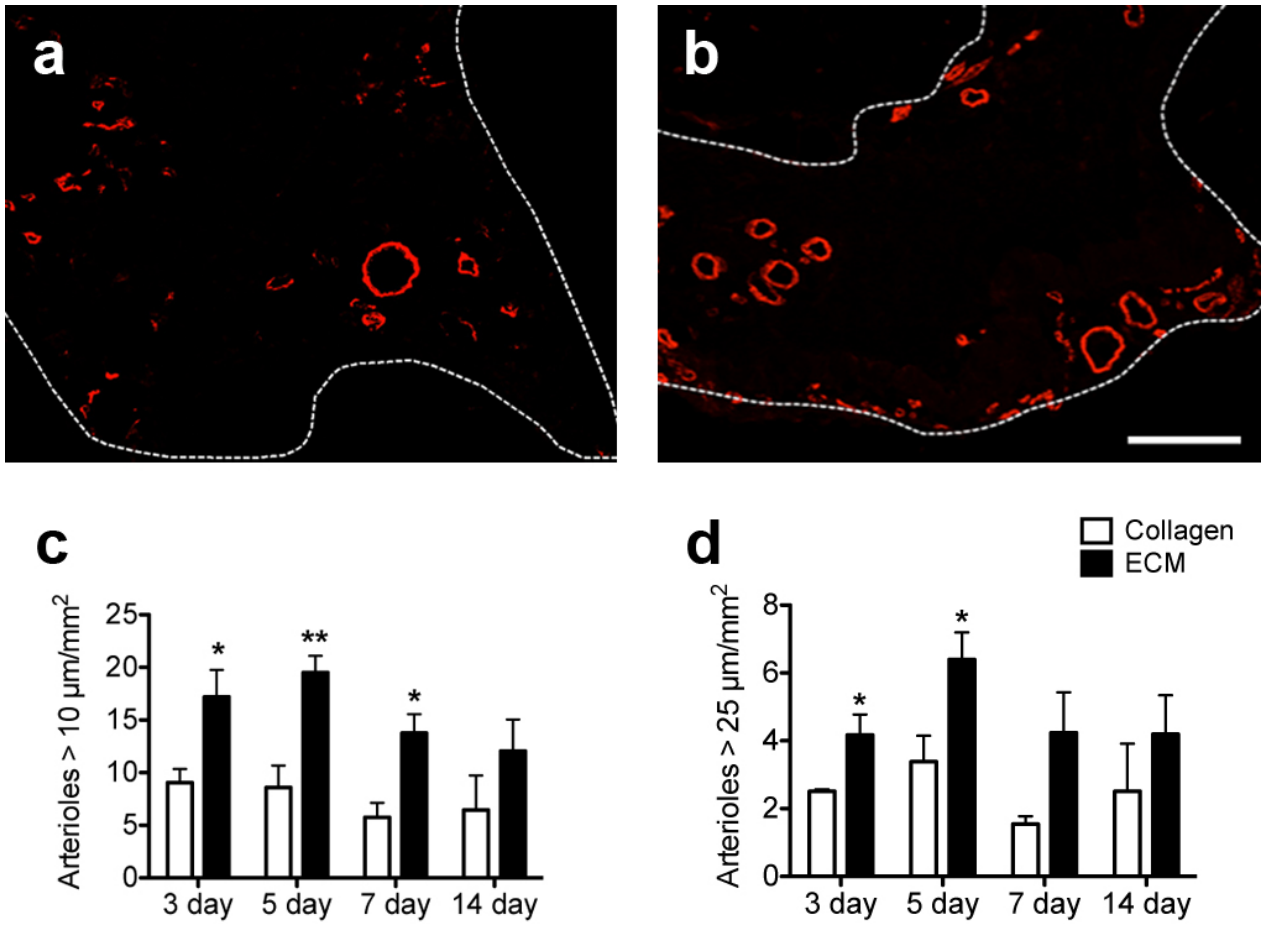

Fig. 6. Quantification of arterioles. Collagen **(a)** and skeletal muscle matrix **(b)** injection regions stained with anti-alpha-SMA (red) to determine arteriole formation. Vessels with a clear lumen are seen within the injection region at 5 d. The area of injection is separated from the skeletal muscle tissue by a dotted white line. Scale bar at 100 µm. Quantification of the vessel density at 3, 5, 7 and 14 d for vessels with a lumen > 10 µm **(c)** or > 25 µm **(d)** demonstrated that the skeletal muscle matrix increased neovascularization. Vessels were, on average, larger in the skeletal muscle matrix when compared to collagen.

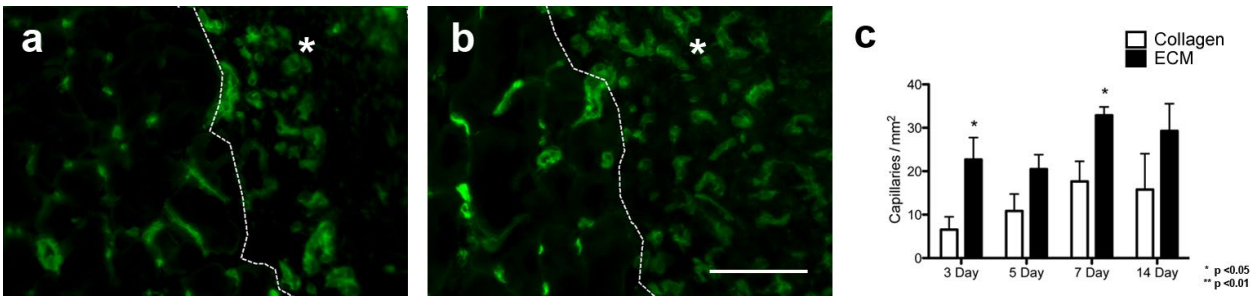

Fig. 7. Quantification of endothelial cell recruitment. Collagen **(a)** and skeletal muscle matrix **(b)** injection regions stained with isolectin (green) to assess endothelial cell infiltration at 5 days. Scale bar at 100 µm. * and dotted line denote area of material. **(c)**. Endothelial cell infiltration at 3, 5, 7 and 14 d was similar across all four time points, but was significantly greater in the skeletal muscle matrix injection region at 3 and 7 d post-injection.

2009), the liquid skeletal muscle matrix assembled into a fibrous scaffold once *in vivo* (Fig. 4c). To assess the microarchitecture of the skeletal muscle matrix hydrogel, the material was injected subcutaneously, and excised after 20 min. SEM demonstrated that the matrix forms a porous, fibrous scaffold, both *in vitro* and *in vivo*, that is composed of fibers on the nano- and micro-scale (Fig. 5).

Cellular infiltration and neovascularization

Upon confirmation that the material was able to assemble upon injection, we next examined the skeletal muscle matrix hydrogel in a rat hindlimb ischemia model to assess its potential for treating PAD. One week post-hindlimb ischemia, either skeletal muscle matrix or collagen was injected intramuscularly below the site of femoral artery

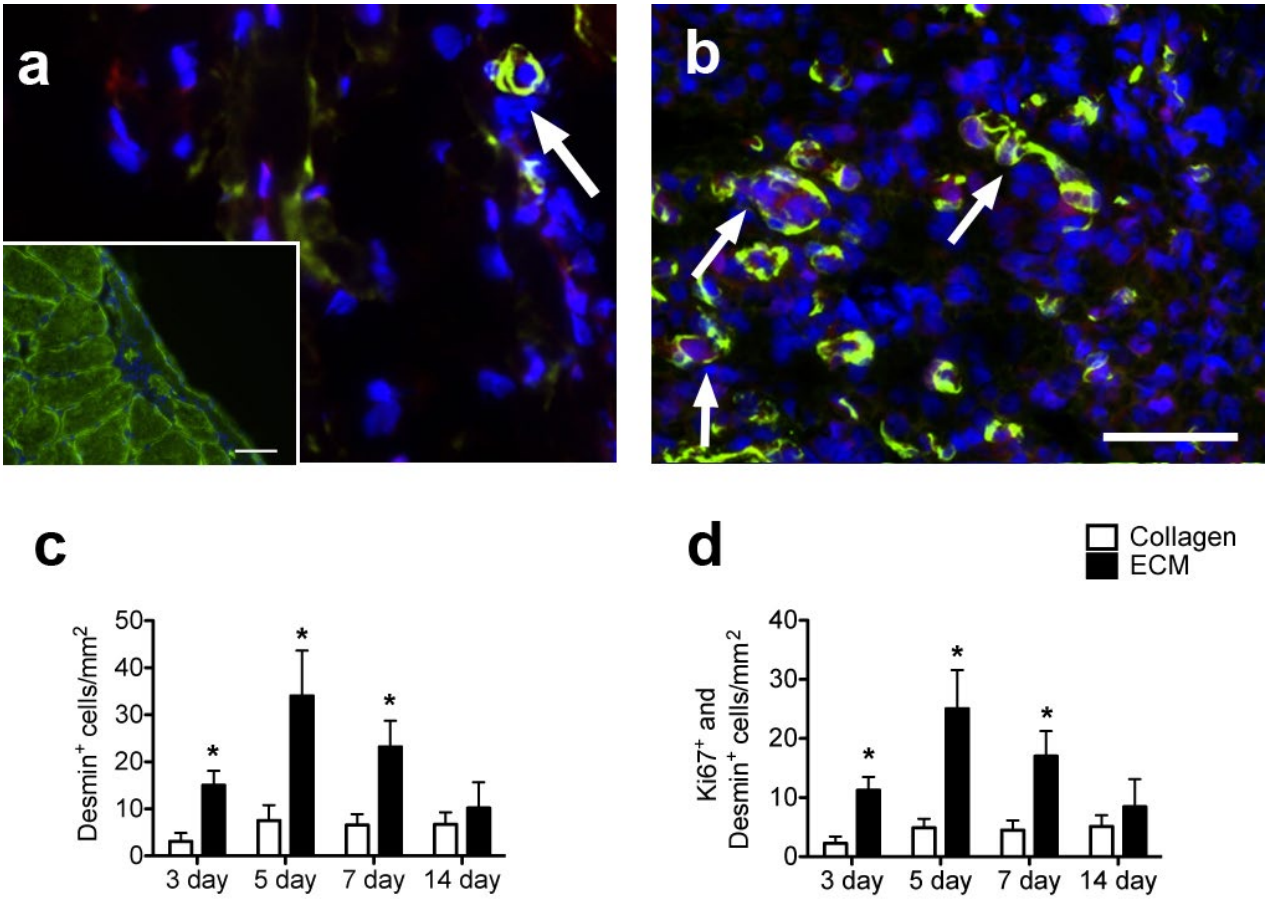

Fig. 8. Proliferating muscle cell recruitment. Collagen injection region **(a)** and skeletal muscle matrix injection **(b)** region at 5 d with desmin-stained cells (green) co-labeled with Ki67 (red). Arrows denote desmin and Ki67 positive cells. Scale bar at 20 μm. Insert shows positive desmin staining of healthy skeletal muscle, scale bar at 100 μm. **(c)** Quantification of desmin-positive cells in the skeletal muscle matrix compared to collagen normalized to area. Note that there are significantly more desmin-positive cells in the skeletal muscle matrix. **(d)** Of these desmin-positive cells, a majority of the cells are proliferating as seen by Ki67 co-labeling.

resection. At 3, 5, 7 or 14 d post-injection, the muscle was harvested to determine cellular infiltration. The hydrogel was still present at all time points, although it had significantly degraded by day 14. At each time point, we assessed the amount of neovascularization, which would be critical to treat the ischemic tissue, as well as the number of muscle cells and muscle progenitors, which could aid in repair of the damaged tissue.

To determine whether the acellular scaffold would support new vessel formation *in vivo*, smooth muscle cells in collagen (Fig. 6a) and skeletal muscle matrix (Fig. 6b) injected regions were labeled via immunohistochemistry. Arteriole density was significantly greater in the skeletal muscle matrix injection region compared to collagen at 3, 5 and 7 d post-injection (Fig. 6c), with many of the vessels having an average diameter greater than 25 μm (Fig. 6d). While not significant, there was still a distinct trend towards an increase in vasculature at day 14 following injection of the skeletal muscle matrix hydrogel. Additionally, endothelial cell infiltration was measured in collagen (Fig. 7a), and skeletal muscle matrix (Fig. 7b) injection regions. Endothelial cell density was found to be similar across all four time points, but was significantly greater in the skeletal muscle matrix injection region at 3 and 7 d post-injection (Fig. 7c).

In PAD and CLI, patients often suffer from general muscle fatigue and atrophy, and therefore, in addition to increasing vascularization, restoring muscle mass would also be beneficial. We therefore sought to determine whether muscle cells were also recruited to the injection site using staining against desmin (Fig. 8a and b). The desmin positive cells were also co-stained for Ki67, a marker for proliferation, as denoted by the arrows in Fig. 8 (Bruey *et al.*, 2010; Diniz *et al.*, 2011; Scholzen and Gerdes, 2000). The skeletal muscle matrix recruited significantly more desmin-positive cells when compared to the collagen matrix at 3, 5 and 7 d post-injection, a trend that continued at day 14 (Fig. 8c). Moreover, the majority of cells expressing desmin also were Ki67 positive, indicating proliferating muscle cells were infiltrating the injection region (Fig. 8d). The number of Ki67 and desmin-positive cells was significantly increased at 3, 5 and 7 d post-injection, with the same trend at day 14. Cell infiltration was further assessed using MyoD as a marker for the potential recruitment of activated satellite cells (Cooper *et al.*, 1999; Megeney *et al.*, 1996). There was a low number

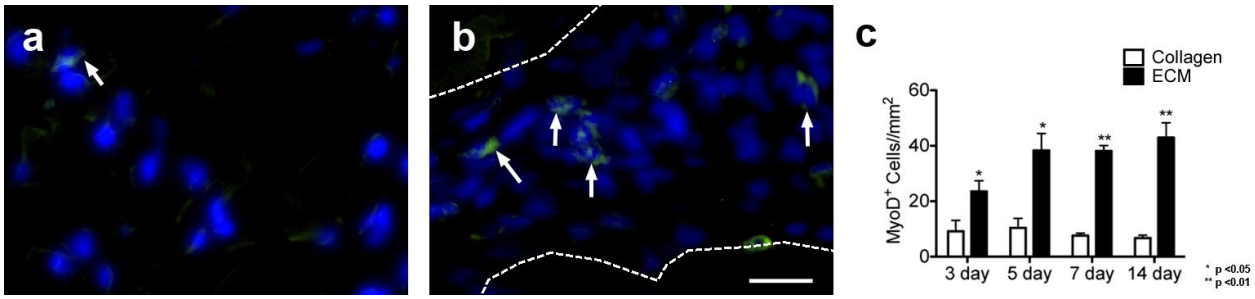

Fig. 9. Muscle progenitor infiltration. MyoD positive cells (green) in collagen **(a)** and skeletal muscle matrix **(b)** injection regions at 5 d. Area of injection is denoted by the dotted line and white arrows indicate MyoD positive cells. Scale bar at 20 μm. **(c)** Graph of MyoD-positive cells normalized to the area for the injection region. The number of MyoD-positive cells was significantly higher in the skeletal muscle matrix regions at all time-points.

of MyoD-positive cells recruited into the injection region of both materials at the examined time points; however, there was a statistically significant increase in MyoD-positive cells in the skeletal muscle matrix (Fig. 9). The MyoD staining was prevalently perinuclear, which has been shown in other studies (Hidestrand *et al.*, 2008; Yamamoto *et al.*, 2008).

Discussion

Similar to myocardial infarction (MI), which is also a result of atherosclerosis, PAD has a large population of affected individuals, with an estimated 27 million suffering from PAD in Europe and North America (Belch *et al.*, 2003). Despite recent medical advances and the advent of tissue engineering strategies, revascularization through surgical or endovascular intervention, remains the only treatment. This is further complicated by the fact that approximately 40 % of patients with CLI, the most severe form of PAD, are not candidates for revascularization procedures (Sprengers *et al.*, 2008), and that revascularization has limited benefit when the PAD is diffuse or below the knee. This corresponds to approximately 120,000 leg amputations in the US and 100,000 in the European Union each year (Lawall *et al.*, 2010). There is therefore a pressing need for the development of new therapies for treating PAD and CLI.

Alternative therapies for PAD and CLI have largely mirrored the attempts for MI and heart failure, including cell transplantation and angiogenic growth factor therapy (Fadini *et al.*, 2010; Menasché, 2010; Tongers *et al.*, 2008). The goal of these therapies has been to increase vascularization of the ischemic limb so that perfusion is sufficient for wound healing to occur, and to resolve pain at rest, thereby also preventing limb amputations. Biomaterial-based strategies have recently been explored. Currently, only poly(d,l-lactide-co-glycolide) (PLGA), collagen-fibronectin, alginate, gelatin, fibrin, and peptide amphiphiles have been examined (Doi *et al.*, 2007; Jay *et al.*, 2008; Kong *et al.*, 2008; Layman *et al.*, 2007; Lee *et al.*, 2010; Ruvinov *et al.*, 2010; Silva and Mooney, 2007; Webber *et al.*, 2011). PLGA microspheres in alginate hydrogels have been utilized to deliver vascular endothelial growth factor (VEGF) (Lee *et al.*, 2010), and alginate hydrogels have been explored for delivery of hepatocyte growth factor (HGF) (Ruvinov *et al.*, 2010), VEGF (Silva and Mooney, 2007), and pDNA encoding for VEGF (Kong *et al.*, 2008). Alginate microspheres within an injectable collagen matrix have also been used to deliver stromal cell-derived factor-1 (SDF-1) (Kuraitis *et al.*, 2011), while VEGF-loaded alginate microparticles in a collagen-fibronectin scaffold were used to deliver endothelial cells (Jay *et al.*, 2008). Gelatin hydrogels have been employed to deliver basic fibroblast growth factor (bFGF) (Doi *et al.*, 2007; Layman *et al.*, 2007), and fibrin scaffolds were utilized to deliver bFGF and granulocyte-colony stimulating factor (G-CSF) along with bone marrow cells. More recently, VEGF-mimetic peptides were delivered using assembling peptide amphiphiles (Webber *et al.*, 2011). Each of these studies demonstrated enhanced cell transplantation and/or enhanced growth factor/gene delivery with resulting enhancements in neovascularization.

While each of the materials currently explored for treating PAD have been used extensively as tissue engineering scaffolds, they do not mimic the extracellular microenvironment of the skeletal muscle they are intended to treat. The native ECM is a complex combination of fibrous proteins and proteoglycans that can affect many aspects of cellular behavior. Therefore, to regenerate tissue, an ideal scaffold will mimic this native microenvironment. We therefore sought to develop an injectable hydrogel derived from skeletal muscle ECM, which would mimic the native biochemical cues, as well as be amenable to minimally invasive, injectable procedures, which would be advantageous for treating PAD and CLI. While the material may also have potential to be used as a delivery vehicle combined with cells and/or growth factors, we studied the material as an acellular stand-alone therapy, which could be used to recruit endogenous cells for neovascularization and repair. We utilized a porcine source of skeletal muscle matrix, as this is the most likely source for a commercial product. Xenogeneic decellularized extracellular matrices have been shown to be biocompatible upon removal of the cellular antigens, and are currently utilized in the clinic for a number of surgical repair applications (Badylak *et al.*, 2009; Badylak and Gilbert, 2008).

We found that our liquid version of skeletal muscle matrix was able to form a porous scaffold upon injection,

which should promote cellular infiltration to the damaged area (Jeon *et al.*, 2011; Sundararaghavan *et al.*, 2010). From previous mass spectrometry data, we did not see the presence of remnant growth factors (DeQuach *et al.*, 2010), and the decellularization and subsequent processing into the hydrogel form decreases the probability of their presence; however, this has not been specifically tested and small amounts of residual growth factors may be possible. We assessed the mitogenic properties of the degradation products of this matrix on smooth muscle cells, a relevant cell type for vascularization. The skeletal muscle matrix degradation fragments induced a higher proliferation rate compared to collagen. Other studies have also demonstrated mitogenic activity with extracellular matrix degradation products (Reing *et al.*, 2009). Care should however be taken when attempting to directly correlate these *in vitro* results to the *in vivo* environment as the majority of these studies, including the study herein, have used pepsin, which would not generate the same ECM degradation products *in vivo*. These *in vitro* studies, however, provided promising evidence that the injectable skeletal muscle matrix scaffold may induce neovascularization *in vivo*. We, therefore, assessed the ability of this new scaffold to induce neovascularization in a rat hindlimb ischemia model compared to collagen, which is the predominant component of the skeletal muscle matrix and a commonly utilized scaffold. Not only was the vessel density higher in the skeletal muscle matrix, but there were significantly more large-diameter vessels greater than 25 μm, indicating maturation of the vasculature. Additionally, significance was seen as early as 3 d post-injection, demonstrating the fast rate of vascularization. However, it must be noted that these effects were only studied in the biomaterial, and not in the surrounding tissues. In PAD, the formation of new blood vessels will be critical to treat the ischemic tissue. The presence of more mature vasculature might indicate permanence of the formed vessels, which would be important to getting a vascular supply as quickly as possible to the ischemic region, and to maintain blood flow (Banker and Goslin, 1998).

In addition to treating the ischemic environment, increasing muscle mass would be beneficial in a therapy for PAD and CLI as patients often suffer with muscle fatigue and atrophy. Previously, we had demonstrated that the liquid form of decellularized skeletal muscle, when utilized as a coating for cell culture, increased skeletal myoblast differentiation compared to collagen coatings (DeQuach *et al.*, 2010), suggesting that this material provides tissue-specific biochemical cues to recapitulate the skeletal muscle microenvironment. In this study, we first examined whether the degradation products of the skeletal muscle matrix scaffold would promote proliferation of skeletal myoblasts *in vitro*. We demonstrated that the degradation products of this scaffold increased myoblast proliferation compared to collagen, which is consistent with literature demonstrating the inhibitory effect of collagen on smooth muscle cells and fibroblasts (Koyama *et al.*, 1996; Rhudy and McPherson, 1988). We next sought to assess the infiltration of muscle cells into the scaffold in the hindlimb ischemia model. We measured the number of desmin- and MyoD-positive cells that were recruited into the skeletal muscle matrix scaffold compared to collagen. Desmin, a muscle specific protein, confirms that the cells that infiltrated were from a myogenic origin; however, this may also stain for smooth muscle cells. MyoD, on the other hand, is a specific striated muscle regulatory transcription factor, which coordinates the myogenic program in differentiating myoblasts (Kanisicak *et al.*, 2009; Lee *et al.*, 2000; Wada *et al.*, 2002). We found that there were a significantly higher number of muscle cell types in the skeletal muscle matrix, and that many of these cells were also proliferating. The MyoD-positive cells also indicate that immature progenitor cell types are recruited to the skeletal muscle matrix. While some caution should be taken when directly extrapolating *in vitro* results to the *in vivo* setting, it is possible that collagen may have inhibited proliferation of infiltrating cells as described above. The presence of these MyoD-positive and desmin-positive muscle cells indicate that the skeletal muscle scaffold is recruiting relevant cell types that may aid in the regeneration of the damaged muscle, in addition to treating the ischemic tissue. However, future studies to assess functional benefit, and studies in a larger animal model will be critical prior to translation of this therapy to the clinic. For instance, regional injection sites might play an important role for functional benefit, and multiple injections might be needed. An additional limitation of using a small animal model is that the 150 μL injection spreads through most of the tissue, and thus examining multiple injection site locations is challenging.

In this study, we demonstrate the potential of an acellular, biomaterial-only therapy for treating PAD. Previous biomaterial strategies for PAD have only utilized scaffolds to enhance cell or growth factor therapy (Doi *et al.*, 2007; Jay *et al.*, 2008; Kong *et al.*, 2008; Layman *et al.*, 2007; Lee *et al.*, 2010; Ruvinov *et al.*, 2010; Silva and Mooney, 2007). However, a lone biomaterial therapy has several benefits, which may allow it to reach patients sooner, including the potential to be an off-the-shelf treatment without the complications that both cells and growth factors can add. To increase its therapeutic benefit, the matrix also has the potential to be used in conjunction with cell or growth factor therapy as these components could also be added to the biomaterial prior to injection. To create a material that could be easily prepared in the clinic, we also developed a method that allowed for long-term storage of the injectable skeletal muscle matrix scaffold, with only sterile water required to resuspend it immediately prior to use.

Conclusions

The results of this study indicate that an injectable skeletal muscle matrix scaffold may be a potential new biomaterial-only therapy for treating PAD. In this study, we demonstrate that decellularized skeletal muscle ECM can be processed to form an injectable matrix material, which assembles into a porous and fibrous scaffold *in vivo*. We show that degradation products of the material induce proliferation of smooth muscle cells and skeletal myoblasts *in vitro*. We further observed that the injected scaffold increased neovascularization and infiltration of muscle cells within

the biomaterial compared to collagen, suggesting that it may improve neovascularization in PAD as well as treat the associated muscle atrophy. Future long-term studies, including those in a larger animal, and studies to assess functional recovery, will be critical prior to translation; however, this study demonstrates proof-of-concept for treating PAD and CLI with an injectable scaffold derived from decellularized skeletal muscle ECM.

Acknowledgements

This research was funded by the National Institutes of Health (NIH) Director's New Innovator Award Program (K.L.C., DP2OD004309), which is part of the NIH Roadmap for Medical Research. F.S. would like to acknowledge CIRM and NIH grants for research funding and support. J.A.D. would like to acknowledge the California Institute for Regenerative Medicine (CIRM) under the UCSD Interdisciplinary Stem Cell Research and Training Program for a pre-doctoral fellowship (TG-01154), as well as the Telemedicine & Advanced Technology Research Center (TATRC) for additional support. The authors would also like to acknowledge Carolina Rogers for her assistance with harvesting skeletal muscle tissue, Anthony Monteforte for sectioning, Ryan Anderson for his aid with SEM, and Valeria Mezzano for helpful discussion. We wish to confirm that there are no known conflicts of interest associated with this publication and there has been no significant financial support for this work that could have influenced its outcome.

References

Alev C, Ii M, Asahara T (2011) Endothelial progenitor cells: a novel tool for the therapy of ischemic diseases. Antioxid Redox Signal **15**: 949-965.

Bach AD, Arkudas A, Tjiawi J, Polykandriotis E, Kneser U, Horch RE, Beier JP (2006) A new approach to tissue engineering of vascularized skeletal muscle. J Cell Mol Med **10**: 716-726.

Badylak SF (2007) The extracellular matrix as a biologic scaffold material. Biomaterials **28**: 3587-3593.

Badylak SF, Gilbert TW (2008) Immune response to biologic scaffold materials. Semin Immunol **20**: 109-116.

Badylak SF, Park K, Peppas N, McCabe G, Yoder M (2001) Marrow-derived cells populate scaffolds composed of xenogeneic extracellular matrix. Exp Hematol **29**: 1310-1318.

Badylak SF, Freytes DO, Gilbert TW (2009) Extracellular matrix as a biological scaffold material: Structure and function. Acta Biomater **5**: 1-13.

Banker G, Goslin K (1998) Culturing Nerve Cells, 2nd edition, MIT Press, Cambridge, MA, pp 68-69.

Beattie AJ, Gilbert TW, Guyot JP, Yates AJ, Badylak SF (2008) Chemoattraction of progenitor cells by remodeling extracellular matrix scaffolds. Tissue Eng Part A **15**: 1119-1125.

Belch JJ, Topol EJ, Agnelli G, Bertrand M, Califf RM, Clement DL, Creager MA, Easton JD, Gavin JR 3rd, Greenland P, Hankey G, Hanrath P, Hirsch AT, Meyer J, Smith SC, Sullivan F, Weber MA (2003) Critical issues in peripheral arterial disease detection and management: a call to action. Arch Intern Med **163**: 884-892.

Bhang SH, Kim JH, Yang HS, La WG, Lee TJ, Kim GH, Kim HA, Lee M, Kim BS (2011) Combined gene therapy with hypoxia-inducible factor-1alpha and heme oxygenase-1 for therapeutic angiogenesis. Tissue Eng Part A **17**: 915-926.

Bruey JM, Kantarjian H, Ma W, Estrov Z, Yeh C, Donahue A, Sanders H, O'Brien S, Keating M, Albitar M (2010) Circulating Ki-67 index in plasma as a biomarker and prognostic indicator in chronic lymphocytic leukemia. Leuk Res **34**: 1320-1324.

Chan YC, Cheng SW (2011) Drug-eluting stents and balloons in peripheral arterial disease: evidence so far. Int J Clin Pract **65**: 664-668.

Christman KL, Vardanian AJ, Fang Q, Sievers RE, Fok HH, Lee RJ (2004) Injectable fibrin scaffold improves cell transplant survival, reduces infarct expansion, and induces neovasculature formation in ischemic myocardium. J Am Coll Cardiol **44**: 654-660.

Cooper RN, Tajbakhsh S, Mouly V, Cossu G, Buckingham M, Butler-Browne GS (1999) *In vivo* satellite cell activation via Myf5 and MyoD in regenerating mouse skeletal muscle. J Cell Sci **112**: 2895-2901.

Crapo PM, Gilbert TW, Badylak SF (2011) An overview of tissue and whole organ decellularization processes. Biomaterials **32**: 3233-3243.

Dattilo PB, Casserly IP (2011) Critical limb ischemia: endovascular strategies for limb salvage. Prog Cardiovasc Dis **54**: 47-60.

DeQuach JA, Mezzano V, Miglani A, Lange S, Keller GM, Sheikh F, Christman KL (2010) Simple and high yielding method for preparing tissue specific extracellular matrix coatings for cell culture. PLoS One **5**: e13039.

Diniz G, Aktas S, Turedi A, Temir G, Ortac R, Vergin C (2011) Telomerase reverse transcriptase catalytic subunit expression and proliferation index in Wilms tumor. Tumour Biol **32**: 761-767.

Doi K, Ikeda T, Marui A, Kushibiki T, Arai Y, Hirose K, Soga Y, Iwakura A, Ueyama K, Yamahara K, Itoh H, Nishimura K, Tabata Y, Komeda M (2007) Enhanced angiogenesis by gelatin hydrogels incorporating basic fibroblast growth factor in rabbit model of hind limb ischemia. Heart Vessels **22**: 104-108.

Fadini GP, Agostini C, Avogaro A (2010) Autologous stem cell therapy for peripheral arterial disease meta-analysis and systematic review of the literature. Atherosclerosis **209**: 10-17.

Gilbert TW, Sellaro TL, Badylak SF (2006) Decellularization of tissues and organs. Biomaterials **27**: 3675-3683.

Gupta R, Losordo DW (2011) Cell therapy for critical limb ischemia: moving forward one step at a time. Circ Cardiovasc Interv **4**: 2-5.

Hidestrand M, Richards-Malcolm S, Gurley CM, Nolen G, Grimes B, Waterstrat A, Zant GV, Peterson CA (2008) Sca-1-expressing nonmyogenic cells contribute to fibrosis in aged skeletal muscle. J Gerontol A Biol Sci Med Sci **63**: 566-579.

Jay SM, Shepherd BR, Bertram JP, Pober JS, Saltzman WM (2008) Engineering of multifunctional gels integrating highly efficient growth factor delivery with endothelial cell transplantation. FASEB J **22**: 2949-2956.

Jeon O, Krebs M, Alsberg E (2011) Controlled and sustained gene delivery from injectable, porous PLGA scaffolds. J Biomed Mater Res A **98**: 72-79.

Kanisicak O, Mendez JJ, Yamamoto S, Yamamoto M, Goldhamer DJ (2009) Progenitors of skeletal muscle satellite cells express the muscle determination gene, MyoD. Dev Biol **332**: 131-141.

Kawamoto A, Katayama M, Handa N, Kinoshita M, Takano H, Horii M, Sadamoto K, Yokoyama A, Yamanaka T, Onodera R, Kuroda A, Baba R, Kaneko Y, Tsukie T, Kurimoto Y, Okada Y, Kihara Y, Morioka S, Fukushima M, Asahara T (2009) Intramuscular transplantation of G-CSF-mobilized CD34(+) cells in patients with critical limb ischemia: a phase I/IIa, multicenter, single-blinded, dose-escalation clinical trial. Stem Cells **27**: 2857-2864.

Kong HJ, Kim ES, Huang YC, Mooney DJ (2008) Design of biodegradable hydrogel for the local and sustained delivery of angiogenic plasmid DNA. Pharm Res **25**: 1230-1238.

Koyama H, Raines EW, Bornfeldt KE, Roberts JM, Ross R (1996) Fibrillar collagen inhibits arterial smooth muscle proliferation through regulation of Cdk2 inhibitors. Cell **87**: 1069-1078.

Kuraitis D, Zhang P, Zhang Y, Padavan DT, McEwan K, Sofrenovic T, McKee D, Zhang J, Griffith M, Cao X, Musaro A, Ruel M, Suuronen EJ (2011) A stromal cell-derived factor-1 releasing matrix enhances the progenitor cell response and blood vessel growth in ischaemic skeletal muscle. Eur Cell Mater **22**: 109-123.

Lawall H, Bramlage P, Amann B (2010) Stem cell and progenitor cell therapy in peripheral artery disease. A critical appraisal. Thromb Haemost **103**: 696-709.

Layman H, Spiga MG, Brooks T, Pham S, Webster KA, Andreopoulos FM (2007) The effect of the controlled release of basic fibroblast growth factor from ionic gelatin-based hydrogels on angiogenesis in a murine critical limb ischemic model. Biomaterials **28**: 2646-2654.

Layman H, Rahnemai-Azar AA, Pham SM, Tsechpenakis G, Andreopoulos FM (2011) Synergistic angiogenic effect of codelivering fibroblast growth factor 2 and granulocyte-colony stimulating factor from fibrin scaffolds and bone marrow transplantation in critical limb ischemia. Tissue Eng Part A **17**: 243-254.

Lee JY, Qu-Petersen Z, Cao B, Kimura S, Jankowski R, Cummins J, Usas A, Gates C, Robbins P, Wernig A, Huard J (2000) Clonal isolation of muscle-derived cells capable of enhancing muscle regeneration and bone healing. J Cell Biol **150**: 1085-1100.

Lee J, Bhang SH, Park H, Kim BS, Lee KY (2010) Active blood vessel formation in the ischemic hindlimb mouse model using a microsphere/hydrogel combination system. Pharm Res **27**: 767-774.

Li F, Li W, Johnson S, Ingram D, Yoder M, Badylak S (2004) Low-molecular-weight peptides derived from extracellular matrix as chemoattractants for primary endothelial cells. Endothelium **11**: 199-206.

Lutolf MP, Hubbell JA (2005) Synthetic biomaterials as instructive extracellular microenvironments for morphogenesis in tissue engineering. Nat Biotechnol **23**: 47-55.

Manzi M, Palena L, Cester G (2011) Endovascular techniques for limb salvage in diabetics with crural and pedal disease. J Cardiovasc Surg **52**: 485-492.

Megeney LA, Kablar B, Garrett K, Anderson JE, Rudnicki MA (1996) MyoD is required for myogenic stem cell function in adult skeletal muscle. Genes Dev **10**: 1173-1183.

Menasché P (2010) Cell therapy for peripheral arterial disease. Curr Opin Mol Ther **12**: 538-545.

Merritt EK, Hammers DW, Tierney M, Suggs LJ, Walters TJ, Farrar RP (2010) Functional assessment of skeletal muscle regeneration utilizing homologous extracellular matrix as scaffolding. Tissue Eng Part A **16**: 1395-1405.

Numata S, Fujisato T, Niwaya K, Ishibashi-Ueda H, Nakatani T, Kitamura S (2004) Immunological and histological evaluation of decellularized allograft in a pig model: comparison with cryopreserved allograft. J Heart Valve Dis **13**: 984-990.

Ott HC, Matthiesen TS, Goh SK, Black LD, Kren SM, Netoff TI, Taylor DA (2008) Perfusion-decellularized matrix: using nature's platform to engineer a bioartificial heart. Nat Med **14**: 213-221.

Reing JE, Zhang L, Myers-Irvin J, Cordero KE, Freytes DO, Heber-Katz E, Bedelbaeva K, McIntosh D, Dewilde A, Braunhut SJ, Badylak SF (2009) Degradation products of extracellular matrix affect cell migration and proliferation. Tissue Eng Part A **15**: 605-614.

Rhudy RW, McPherson JM (1988) Influence of the extracellular matrix on the proliferative response of human skin fibroblasts to serum and purified platelet-derived growth factor. J Cell Physiol **137**: 185-191.

Rieder E, Nigisch A, Dekan B, Kasimir MT, Muhlbacher F, Wolner E, Simon P, Weigel G (2006) Granulocyte-based immune response against decellularized or glutaraldehyde cross-linked vascular tissue. Biomaterials **27**: 5634-5642.

Ruvinov E, Leor J, Cohen S (2010) The effects of controlled HGF delivery from an affinity-binding alginate biomaterial on angiogenesis and blood perfusion in a hindlimb ischemia model. Biomaterials **31**: 4573-4582.

Scholzen T, Gerdes J (2000) The Ki-67 protein: from the known and the unknown. J Cell Physiol **182**: 311-322.

Seif-Naraghi SB, Salvatore MA, Schup-Magoffin PJ, Hu DP, Christman KL (2010) Design and characterization of an injectable pericardial matrix gel: a potentially autologous scaffold for cardiac tissue engineering. Tissue Eng Part A **16**: 2017-2027.

Silva EA, Mooney DJ (2007) Spatiotemporal control of vascular endothelial growth factor delivery from injectable hydrogels enhances angiogenesis. J Thromb Haemost **5**: 590-598.

Singelyn JM, DeQuach JA, Seif-Naraghi SB, Littlefield RB, Schup-Magoffin PJ, Christman KL (2009) Naturally derived myocardial matrix as an injectable scaffold for cardiac tissue engineering. Biomaterials **30**: 5409-5416.

Singelyn JM, Sundaramurthy P, Johnson TD, Schup-Magoffin PJ, Hu DP, Faulk DM, Wang J, Mayle KM, Bartels K, Salvatore M, Kinsey AM, Demaria AN, Dib N, Christman KL (2012) Catheter-deliverable hydrogel derived from decellularized ventricular extracellular matrix increases endogenous cardiomyocytes and preserves cardiac function post-myocardial infarction. J Am Coll Cardiol **59**: 751-763.

Sprengers RW, Lips DJ, Moll FL, Verhaar MC (2008) Progenitor cell therapy in patients with critical limb ischemia without surgical options. Ann Surg **247**: 411-420.

Stansby G, Williams R (2011) Angioplasty for treatment of isolated below-the-knee arterial stenosis in patients with critical limb ischemia. Angiology **62**: 357-358.

Sundararaghavan HG, Metter RB, Burdick JA (2010) Electrospun fibrous scaffolds with multiscale and photopatterned porosity. Macromol Biosci **10**: 265-270.

Tongers J, Roncalli JG, Losordo DW (2008) Therapeutic angiogenesis for critical limb ischemia: microvascular therapies coming of age. Circulation **118**: 9-16.

Uriel S, Labay E, Francis-Sedlak M, Moya ML, Weichselbaum RR, Ervin N, Cankova Z, Brey EM (2009) Extraction and assembly of tissue-derived gels for cell culture and tissue engineering. Tissue Eng Part C **15**: 309-321.

Uygun BE, Soto-Gutierrez A, Yagi H, Izamis ML, Guzzardi MA, Shulman C, Milwid J, Kobayashi N, Tilles A, Berthiaume F, Hertl M, Nahmias Y, Yarmush ML, Uygun K (2010) Organ reengineering through development of a transplantable recellularized liver graft using decellularized liver matrix. Nat Med **16**: 814-820.

Valentin JE, Turner NJ, Gilbert TW, Badylak SF (2010) Functional skeletal muscle formation with a biologic scaffold. Biomaterials **31**: 7475-7484.

Wada MR, Inagawa-Ogashiwa M, Shimizu S, Yasumoto S, Hashimoto N (2002) Generation of different fates from multipotent muscle stem cells. Development **129**: 2987-2995.

Webber MJ, Tongers J, Newcomb CJ, Marquardt KT, Bauersachs J, Losordo DW, Stupp SI (2011) Supramolecular nanostructures that mimic VEGF as a strategy for ischemic tissue repair. Proc Natl Acad Sci USA **108**: 13438-13443.

Wolf MT, Daly KA, Reing JE, Badylak SF (2012) Biologic scaffold composed of skeletal muscle extracellular matrix. Biomaterials **33**: 2916-2925.

Yamamoto DL, Csikasz RI, Li Y, Sharma G, Hjort K, Karlsson R, Bengtsson T (2008) Myotube formation on micro-patterned glass: intracellular organization and protein distribution in C2C12 skeletal muscle cells. J Histochem Cytochem **56**: 881-892.

Young DA, Ibrahim DO, Hu D, Christman KL (2011) Injectable hydrogel scaffold from decellularized human lipoaspirate. Acta Biomater **7**: 1040-1049.

Zantop T, Gilbert TW, Yoder MC, Badylak SF (2006) Extracellular matrix scaffolds are repopulated by bone marrow-derived cells in a mouse model of achilles tendon reconstruction. J Orthop Res **24**: 1299-1309.

Discussion with Reviewers

Reviewer I: How would you interpret the decreased proliferation rate observed when cells were grown on a type I collagen substrate (compared to pepsin buffer) and the increased proliferation when grown with the pepsin-digested ECM? How might these results translate to the *in vivo* component?
Authors: All of the cells were cultured on an uncoated surface, and the described effect was seen when the collagen and pepsin were added to the media at very low concentrations (0.05 mg/mL), not as a culture substrate. Although the pepsin and collagen controls were not statistically significant, there is a visible trend. It has been previously shown that the addition of collagen can inhibit smooth muscle and fibroblast proliferation in a fibrillar form. While we think that some caution should be taken when directly extrapolating *in vitro* results to the *in vivo* setting, these results may indicate the collagen was in fact inhibiting proliferation of infiltrating cells.

Reviewer II: Can the choice of ECM matrix scaffold be expanded to other cell types of relevance?
Authors: To regenerate skeletal muscle tissue an ideal scaffold should contain a composition similar to that of the tissue it is trying to replace, which is why skeletal muscle ECM was chosen for this study. Skeletal muscle is known to be composed of muscle cells that fuse and form into fibers, but is also vascularized. Thus, we chose to study skeletal muscle cells as well as smooth muscle and endothelial cell infiltration into the skeletal muscle matrix scaffold.

Reviewer II: What is the functional benefit to organ and kinetic of repair?
Authors: In this initial study we demonstrated increased neovascularization and muscle cell recruitment into the skeletal muscle matrix when compared to collagen hydrogels, demonstrating proof-of-concept for this material in treating PAD. Our results indicate that it has the potential to treat the ischemia as well as muscle atrophy associated with PAD. However, functional recovery and studies in a larger animal model will be critical to properly evaluate this potential therapy prior to translation.